Research Paper

Analytical Modeling of I-beam as a Sandwich Structure

Krzysztof MAGNUCKI, Jerzy LEWINSKI

Institute of Rail Vehicles "TABOR"
Warszawska 181, 61-055 Poznan, Poland
e-mail: jerzy.lewinski@tabor.com.pl

The paper is devoted to an analytical model of I-beam, with consideration of the shear effect. The model is based on the sandwich beam theory. The field displacements and strains are formulated with consideration of a nonlinear hypothesis of flat cross-section deformation of the beam. The governing differential equations for the I-beam are obtained based on the principle of stationary total potential energy. The shear effect of the beam is illustrated for the three-point bending case. The analytical solution is compared to FEM numerical calculation. The results of the analysis are presented in Tables and Figures.

Key words: I-beam; shear deformation; three-point bending; sandwich beam theory.

1. INTRODUCTION

The original model of the beam with transverse shear deformation was formulated by S.P. Timoshenko in 1921. GERE and TIMOSHENKO [1] described in details the shear effect on the stresses and deflection of typical beams. WANG *et al.* [2] presented the shear effect in beams and plates using the nonlinear hypothesis formulated with application of polynomials. HUTCHINSON [3] described the shear coefficients for the Timoshenko beam theory. SONG *et al.* [4] presented analytical solutions of static response of an anisotropic I-beam loaded at its free ends. They used two main coupling mechanisms, i.e. the circumferentially uniform stiffness and circumferentially asymmetric stiffness configurations. The directional properties of the composite materials have been taken into account and the effect of transverse shear on the I-beam static behaviour has been considered. JUNG and LEE [5] analyzed thin-walled composite I-beams. The force-displacement relationship was determined based on the Reissner's semi-complementary energy functional. The effects of warping restraint and transverse shear deformation on the beam static response were investigated. The effects of torsion shear forces in the beam were considered by FATMI [6]. An unchanged shape of the beam cross-section was assumed and the beam theory

based on the displacement model was developed, using the principle of virtual work. ROMANOFF and VARSTA [7] considered bending of the sandwich plates. They replaced a discrete core of the plate with a homogeneous continuum and determined equivalent properties of the plate. BLAAUWENDRAAD [8] considered accuracy and applicability of the Haringx and Engesser theories related to stability of structural members. Final conclusion of the paper recommends to avoid the Haringx theory and to replace it by the Engesser theory for this purpose. DONG et al. [9] formulated the shear correction factors for the Timoshenko beam theory. They dealt only with homogeneous and isotropic beams and used semi-analytical finite element method in order to find static and dynamic response of the considered beam. SHI and VOYIADJIS [10] presented a new beam theory formulated with the sixth-order differential equilibrium equations describing the shear deformable beams. The example solutions have shown that the considered theory is able to depict some boundary layer behaviour in the vicinity of the beam ends and loading points. BECK and SILVA Jr. [11] compared the Euler-Bernoulli and Timoshenko beam theories. In the paper some beam parameters were modeled as parametrized stochastic processes. The problems were solved with the Monte Carlo-Galerkin scheme. In conclusion it was found that both theories give equivalent deterministic responses while the uncertainties with respect to the beam height and elasticity modulus propagate quite differently. KIM [12] theoretically studied the coupled flexural and torsional state of thin-walled composite I-beams of doubly- and mono-symmetric cross-sections using the first-order shear deformation beam theory. A shear deformable beam finite element has been developed for this purpose. The equations describing the object have been derived from the principle of minimum total potential energy. The explicit formulae have been formulated with the use of power series expansions of the displacement components. The results obtained with the help of such an approach have been compared to the ones originated based on the ABAQUS shell elements and the solutions of other researchers. MAGNUCKA-BLANDZI [13, 14] presented generalization of mathematical modeling and dynamic stability of sandwich plates and beams with a metal foam core. Mechanical properties of the isotropic metal foam varied in the direction normal to the middle symmetry plane. The systems of partial differential equations obtained this way have been solved approximately, which allowed to formulate the strength and stability conditions related to particular layers of the systems. SHI and WANG [15] considered an improvement of the third-order shear deformation theories of isotropic plates. LI et al. [16] presented the relationship between the solutions of bending of the functionally graded material beams based on the Levinson beam theory and similar homogenous beams based on the classical beam theory. Transverse shearing in sandwich beams with sinusoidally corrugated cores was researched by MAGNUCKA-BLANDZI et al. [17]. The effect of the shearing on

deflections and critical loads of the sandwich beam were analytically determined and verified numerically. Urbański [18] developed an approach to cross-section analysis based on the finite element method. The 3D strain and stress state of the system was taken into account, meeting the equilibrium and constitutive equations at any point and presented two practical cases of the method application Deflection, rotational angle, bending moment, and shear force of the Levinson beams were computed analytically and compared to the reference homogenous Euler-Bernoulli beams. Magnucki *et al.* [19] presented three-point bending of short beams with symmetrically varying mechanical properties. The problem was solved analytically with the use of the Fourier series and numerically using FEM. Schulz [20] developed an original beam element. The cross section of arbitrary geometry is modeled by two-dimensional finite elements. The displacement shapes of the cross sections are described by the axial functions of their motion. The model effectiveness is estimated based on several examples using linear-elastic materials.

The main goal of the paper is focused on elaboration of an analytical model of I-beam with application of the sandwich beam theory, analytical solution of the problem and FEM numerical calculation in order to compare these both approaches. Application of the analytical sandwich model to I-beam is an original approach to the problem.

2. Analytical model of the I-beam

The Euler-Bernoulli beam theory disregards the deformation caused by the transverse shear. The assumption that the plane cross-section before bending remains plane after the bending eliminates the shear effect. Thus, for analytical modeling of the I-beam the sandwich beam theory is adopted. The hypotheses related to sandwich beams are presented, e.g. by Magnucka-Blandzi [13, 14].

The load scheme of the considered beam is shown in Fig. 1. The beam is subject to pure bending complying with the scheme of the three-point flexural test.
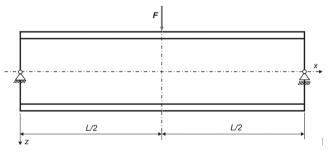

Fig. 1. Three-point bending of the considered I-beam.

The dimensions of the considered I-beam cross-section and the hypothesis of its deformation pattern are depicted in Fig. 2. The displacements resulting from the hypothesis are as follows:

- the upper flange $\left\{-\left(\frac{1}{2}a + t_f\right) \leq z \leq -\frac{1}{2}a\right\}$:

$$(2.1) \qquad u(x, z) = -\left[z\frac{\mathrm{d}w}{\mathrm{d}x} + a\psi_0(x)\right],$$

- the bottom flange $\left\{\frac{1}{2}a \leq z \leq \frac{1}{2}a + t_f\right\}$:

$$(2.2) \qquad u(x, z) = -\left[z\frac{\mathrm{d}w}{\mathrm{d}x} - a\psi_0(x)\right],$$
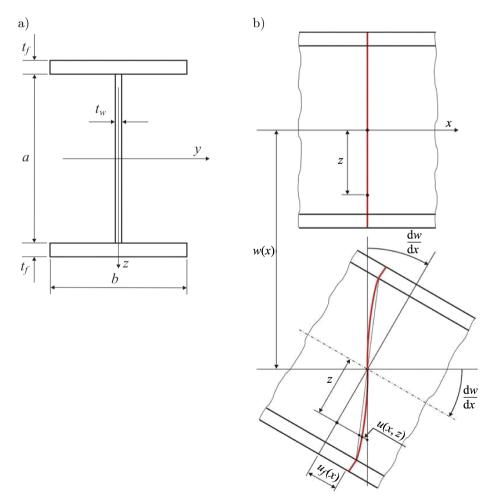

FIG. 2. Cross-section of the I-beam (a) and its deformation (b) – nonlinear hypothesis.

- the web $\left\{ -\frac{1}{2}a \le z \le \frac{1}{2}a \right\}$

(2.3) $$u\left(x, z\right) = -\left\{ z\left[\frac{\mathrm{d}w}{\mathrm{d}x} - 2\psi_0\left(x\right)\right] - a\psi_1\left(x\right)\sin\left(2\pi\frac{z}{a}\right) \right\},$$

where $w(x)$ – deflection, $\psi_0(x) = \frac{u_f(x)}{a}$ and $\psi_1(x)$ – dimensionless functions.
Then, the strains are as follows:

- the upper/bottom flanges

(2.4)
$$\varepsilon_x^{(f-\mathrm{upp})} = \frac{\partial u}{\partial x} = -\left(z\frac{\mathrm{d}^2w}{\mathrm{d}x^2} + a\frac{\mathrm{d}\psi_0}{\mathrm{d}x} \right),$$

$$\varepsilon_x^{(f-\mathrm{low})} = \frac{\partial u}{\partial x} = -\left(z\frac{\mathrm{d}^2w}{\mathrm{d}x^2} - a\frac{\mathrm{d}\psi_0}{\mathrm{d}x} \right),$$

(2.5) $$\gamma_{xz}^{(f)} = \frac{\partial u}{\partial z} + \frac{\mathrm{d}w}{\mathrm{d}x} = 0,$$

- the web

(2.6) $$\varepsilon_x^{(w)} = \frac{\partial u}{\partial x} = -\left\{ z\left[\frac{\mathrm{d}^2w}{\mathrm{d}x^2} - 2\frac{\mathrm{d}\psi_0}{\mathrm{d}x}\right] - a\frac{\mathrm{d}\psi_1}{\mathrm{d}x}\sin\left(2\pi\frac{z}{a}\right) \right\},$$

(2.7) $$\gamma_{xz}^{(w)} = \frac{\partial u}{\partial z} + \frac{\mathrm{d}w}{\mathrm{d}x} = 2\left[\psi_0\left(x\right) + \pi\psi_1\left(x\right)\cos\left(2\pi\frac{z}{a}\right)\right].$$

The elastic strain energy

(2.8) $$U_\varepsilon = U_\varepsilon^{(f)} + U_\varepsilon^{(w)},$$

where

- the elastic strain energy of the flanges

(2.9) $$U_\varepsilon^{(f)} = \frac{E}{2}\int_0^L \left\{ \int_{A_f}\left[\varepsilon_x^{(f-\mathrm{upp})}\right]^2 \mathrm{d}A_f + \int_{A_f}\left[\varepsilon_x^{(f-\mathrm{low})}\right]^2 \mathrm{d}A_f \right\} \mathrm{d}x,$$

where E – Young's modulus, L – length of the beam.

Substitution of the expressions for strains (2.4) into (2.9) gives

$$(2.10)\quad U_\varepsilon^{(f)} = \frac{Eb}{2} \int\limits_0^L \left\{ \int\limits_{-(a/2+t_f)}^{-a/2} \left(z\frac{\mathrm{d}^2 w}{\mathrm{d}x^2} + a\frac{\mathrm{d}\psi_0}{\mathrm{d}x} \right)^2 \mathrm{d}z \right.$$

$$\left. + \int\limits_{a/2}^{a/2+t_f} \left(z\frac{\mathrm{d}^2 w}{\mathrm{d}x^2} - a\frac{\mathrm{d}\psi_0}{\mathrm{d}x} \right)^2 \mathrm{d}z \right\} \mathrm{d}x,$$

and, after integration

$$(2.11)\quad U_\varepsilon^{(f)} = Ea^3 b \int\limits_0^L \left[\frac{1}{12} x_1 \left(3 + 6x_1 + 4x_1^2 \right) \left(\frac{\mathrm{d}^2 w}{\mathrm{d}x^2} \right)^2 \right.$$

$$\left. - x_1 \left(1 + x_1 \right) \frac{\mathrm{d}^2 w}{\mathrm{d}x^2} \frac{\mathrm{d}\psi_0}{\mathrm{d}x} + x_1 \left(\frac{\mathrm{d}\psi_0}{\mathrm{d}x} \right)^2 \right] \mathrm{d}x,$$

where $x_1 = \frac{t_f}{a}$ – dimensionless parameter, a – depth of the web, b – width of the I-beam, t_f – thicknesses of the flanges, t_w – thickness of the web.

- the elastic strain energy of the web

$$(2.12)\quad U_\varepsilon^{(w)} = \frac{1}{2} \int\limits_0^L \left\{ \int\limits_{A_w} \left[\left(E\left(\varepsilon_x^{(w)} \right)^2 + G\left(\gamma_{xz}^{(w)} \right)^2 \right) \right] \mathrm{d}A_w \right\} \mathrm{d}x,$$

where $G = \frac{E}{2(1+\nu)}$ – shear modulus of elasticity, ν – Poisson's ratio.

Substitution of the expressions for strains (2.6) and (2.7) into (2.12) gives, after integration

$$(2.13)\quad U_\varepsilon^{(w)} = \frac{1}{2} a^3 t_w \int\limits_0^L \left[E \cdot \Phi_1 \left(w, \psi_0, \psi_1 \right) + G \cdot \Phi_2 \left(\psi_0, \psi_1 \right) \right] \mathrm{d}x,$$

where

$$\Phi_1 \left(w, \psi_0, \psi_1 \right) = \frac{1}{12} \left(\frac{\mathrm{d}^2 w}{\mathrm{d}x^2} - 2\frac{\mathrm{d}\psi_0}{\mathrm{d}x} \right)^2 - \frac{1}{\pi} \frac{\mathrm{d}^2 w}{\mathrm{d}x^2} \frac{\mathrm{d}\psi_1}{\mathrm{d}x} + \frac{2}{\pi} \frac{\mathrm{d}\psi_0}{\mathrm{d}x} \frac{\mathrm{d}\psi_1}{\mathrm{d}x} + \frac{1}{2} \left(\frac{\mathrm{d}\psi_1}{\mathrm{d}x} \right)^2,$$

$$\Phi_2 \left(\psi_0, \psi_1 \right) = \frac{4}{a^2} \left[\psi_0^2 \left(x \right) + \frac{\pi^2}{2} \psi_1^2 \left(x \right) \right].$$

The work of the load

(2.14)
$$W = \int_0^L qw(x)\,\mathrm{d}x,$$

where q– the intensity of the transverse load.

Based on the theorem of stationary total potential energy

(2.15)
$$\delta\left(U_\varepsilon - W\right) = 0,$$

one obtains three differential equations of equilibrium in the following form:

(2.16) δw)
$$C_{ww}\frac{\mathrm{d}^4 w}{\mathrm{d}x^4} - C_{w\psi_0}\frac{\mathrm{d}^3\psi_0}{\mathrm{d}x^3} - \frac{x_2}{2\pi}\frac{\mathrm{d}^3\psi_1}{\mathrm{d}x^3} = \frac{q}{Ea^3 b},$$

(2.17) $\delta\psi_0$) $C_{w\psi_0}\dfrac{\mathrm{d}^3 w}{\mathrm{d}x^3} - C_{\psi_0\psi_0}\dfrac{\mathrm{d}^2\psi_0}{\mathrm{d}x^2} - \dfrac{x_2}{\pi}\dfrac{\mathrm{d}^2\psi_1}{\mathrm{d}x^2} + \dfrac{2}{1+\nu}x_2\dfrac{\psi_0(x)}{a^2} = 0,$

(2.18) $\delta\psi_1$)
$$\frac{\mathrm{d}^3 w}{\mathrm{d}x^3} - 2\frac{\mathrm{d}^2\psi_0}{\mathrm{d}x^2} - \pi\frac{\mathrm{d}^2\psi_1}{\mathrm{d}x^2} + 2\frac{\pi^3}{1+\nu}\frac{\psi_1(x)}{a^2} = 0,$$

where

$$C_{ww} = \frac{1}{12}\left[2x_1\left(3 + 6x_1 + 4x_1^2\right) + x_2\right], \qquad C_{w\psi_0} = x_1\left(1 + x_1\right) + \frac{1}{6}x_2,$$

$$C_{\psi_0\psi_0} = 2\left(x_1 + \frac{1}{6}x_2\right),$$

and $x_2 = \frac{t_w}{b}$ – dimensionless parameter.

The bending moment of the beam is as follows

(2.19)
$$M_b(x) = E\left[b\int_{-(a/2+t_f)}^{-a/2} z\varepsilon_x^{(f-\mathrm{upp})}\,\mathrm{d}z + t_w\int_{-a/2}^{a/2} z\varepsilon_x^{(w)}\,\mathrm{d}z + b\int_{a/2}^{a/2+t_f} z\varepsilon_x^{(f-\mathrm{low})}\,\mathrm{d}z\right].$$

Substituting the expressions for strains (2.4) and (2.6) and integrating one obtains

(2.20)
$$C_{ww}\frac{\mathrm{d}^2 w}{\mathrm{d}x^2} - C_{w\psi_0}\frac{\mathrm{d}\psi_0}{\mathrm{d}x} - \frac{x_2}{2\pi}\frac{\mathrm{d}\psi_1}{\mathrm{d}x} = -\frac{M_b(x)}{Ea^3 b}.$$

The equations (2.16) and (2.20) are equivalent, therefore the three equations (2.17), (2.18) and (2.20) are governing equations of the I-beam with consideration of the shear effect.

3. Solution of the analytical model for the three-point bending

The I-beam for the three-point bending is shown in Fig. 2. The bending moment described by the Fourier series takes the following form

$$(3.1) \qquad M_b(x) = \frac{2}{\pi^2}\left[\sin(\pi\xi) - \frac{1}{3^2}\sin(3\pi\xi) + \frac{1}{5^2}\sin(5\pi\xi) - ...\right]FL,$$

where $\xi = \frac{x}{L}$ – dimensionless coordinate.

The unknown three functions of the system of equations (2.17), (2.18) and (2.20) are assumed in the following form:

$$(3.2) \qquad w(x) = w_1\sin(\pi\xi) - w_3\sin(3\pi\xi) + w_5\sin(5\pi\xi) - ...,$$

$$(3.3) \qquad \psi_0(x) = \psi_{01}\cos(\pi\xi) - \psi_{03}\cos(3\pi\xi) + \psi_{05}\cos(5\pi\xi) - ...,$$

$$(3.4) \qquad \psi_1(x) = \psi_{11}\cos(\pi\xi) - \psi_{13}\cos(3\pi\xi) + \psi_{15}\cos(5\pi\xi) - ...,$$

where w_k, ψ_{0k}, ψ_{1k} – unknown coefficients of the function for $k = 1, 3, 5, ...$

Substitution of these functions into the differential equations of equilibrium (2.17), (2.18) and (2.20) allows to calculate the coefficients:

$$(3.5) \qquad w_k = \widetilde{w}_k\frac{F\lambda^3}{Eb}, \qquad \psi_{0k} = \widetilde{\psi}_{0k}\frac{F\lambda^2}{Eab}, \qquad \psi_{1k} = \widetilde{\psi}_{1k}\frac{F\lambda^2}{Eab},$$

where

$$\widetilde{w}_k = \frac{2}{(k\pi)^4\,C_{wk}}, \qquad \widetilde{\psi}_{0k} = \frac{2}{(k\pi)^3\,C_{\psi 0k}}, \qquad \widetilde{\psi}_{1k} = \frac{2}{(k\pi)^3\,C_{\psi 1k}},$$

$$C_{wk} = C_{ww} - \frac{\alpha_w}{\alpha_0}, \qquad \alpha_w = C_{w\psi_0}\left(C_{w\psi_0}C_1 - \frac{2}{\pi}x_2\right) + \frac{x_2}{2\pi}C_0,$$

$$\alpha_0 = C_0C_1 - \frac{2}{\pi}x_2, \qquad C_{\psi 0k} = \frac{\alpha_0}{\alpha_{\psi_0}}C_{wk}, \qquad \alpha_{\psi_0} = C_{w\psi_0}C_1 - \frac{x_2}{\pi},$$

$$C_{\psi 1k} = \frac{\alpha_0}{\alpha_{\psi_1}}C_{wk}, \qquad \alpha_{\psi_1} = C_0 - 2C_{w\psi_0}, \qquad C_0 = C_{\psi_0\psi_0} + \frac{2}{\pi^2}\frac{x_2}{1+\nu}\left(\frac{\lambda}{k}\right)^2,$$

$$C_1 = \pi\left[1 + \frac{2}{1+\nu}\left(\frac{\lambda}{k}\right)^2\right],$$

$\lambda = \frac{L}{a}$ – relative length.

The maximum deflection of the I-beam based on the expression (3.2)

$$(3.6) \qquad w_{\max}^{(A-S)} = w\left(\frac{L}{2}\right) = \frac{F\lambda^3}{Eb} \sum_{k=1}^{n} \widetilde{w}_k \sin^2\left(\frac{\pi}{2}k\right).$$

Taking into account the expression (2.4) and (2.6) the normal stress of the I-beam takes a form:

- the upper/bottom flanges

$$(3.7) \qquad \sigma_x^{(f)} = -E\left(z\frac{\mathrm{d}^2 w}{\mathrm{d}x^2} \pm a\frac{\mathrm{d}\psi_0}{\mathrm{d}x}\right),$$

- the web

$$(3.8) \qquad \sigma_x^{(w)} = -E\left\{z\left[\frac{\mathrm{d}^2 w}{\mathrm{d}x^2} - 2\frac{\mathrm{d}\psi_0}{\mathrm{d}x}\right] - a\frac{\mathrm{d}\psi_1}{\mathrm{d}x}\sin\left(2\pi\frac{z}{a}\right)\right\}.$$

Thus, the maximum of normal stress occurs for $x = \frac{L}{2}$ and $z = \mp\left(\frac{a}{2} + t_f\right)$:

$$(3.9) \qquad \sigma_{\max}^{(A-S)} = \frac{F\lambda}{ab} \sum_{k=1}^{n} \widetilde{\sigma}_k \sin^2\left(\frac{\pi}{2}k\right),$$

where $\widetilde{\sigma}_k = \frac{1}{(k\pi)^2}\left(\frac{1+2x_1}{C_{wk}} - \frac{2}{C_{\psi_0 k}}\right)$.

Taking into account the expression (2.7), the shear stress of the I-beam takes a form

$$(3.10) \qquad \tau_{xz}^{(w)} = 2G\left[\psi_0\left(x\right) + \pi\psi_1\left(x\right)\cos\left(2\pi\frac{z}{a}\right)\right],$$

from which

$$(3.11) \quad \tau_{xz}^{(w)}\left(z\right) = \frac{1}{1+\nu}\left[\sum_{k=1}^{n} \widetilde{\psi}_{0k}\sin\left(\frac{\pi}{2}k\right) + \pi\cos\left(2\pi\frac{z}{a}\right)\sum_{k=1}^{n} \widetilde{\psi}_{1k}\sin\left(\frac{\pi}{2}k\right)\right]\frac{F\lambda^2}{ab}.$$

Thus, maximum of the shear stress occurs for $z = 0$

$$(3.12) \quad \tau_{\max}^{(A-S)} = \tau_{\max}^{(w)} = \frac{1}{1+\nu}\left[\sum_{k=1}^{n} \widetilde{\psi}_{0k}\sin\left(\frac{\pi}{2}k\right) + \pi\sum_{k=1}^{n} \widetilde{\psi}_{1k}\sin\left(\frac{\pi}{2}k\right)\right]\frac{F\lambda^2}{ab},$$

and minimum of the shear stress occurs for $z = \mp a/2$

$$(3.13) \quad \tau_{\min}^{(A-S)} = \tau_{\min}^{(w)} = \frac{1}{1+\nu}\left[\sum_{k=1}^{n} \widetilde{\psi}_{0k}\sin\left(\frac{\pi}{2}k\right) - \pi\sum_{k=1}^{n} \widetilde{\psi}_{1k}\sin\left(\frac{\pi}{2}k\right)\right]\frac{F\lambda^2}{ab}.$$

The deflection and normal stress of the I-beam for the three-point bending under the Euler-Bernoulli beam theory are as follows:

$$(3.14) \qquad w_{\max}^{(E-B)} = \frac{1}{48C_{ww}} \frac{F\lambda^3}{Eb}, \qquad \sigma_{\max}^{(E-B)} = \frac{1+2x_1}{8C_{ww}} \frac{F\lambda}{ab}.$$

Taking into account the work of GERE and TIMOSHENKO [1], the shear stress of the I-beam is

$$(3.15) \qquad \tau_{\max}^{(G-T)} = \frac{4x_1(1+x_1)+x_2}{16C_{ww}x_2} \frac{F}{ab}, \qquad \tau_{\min}^{(G-T)} = \frac{x_1(1+x_1)}{4C_{ww}x_2} \frac{F}{ab}.$$

The detailed analysis is carried out for the example steel I-beam: $a = 170$ mm, $b = 200$ mm, $t_f = 15$ mm, $t_w = 9$ mm, $\nu = 0.3$, $E = 2 \cdot 10^5$ MPa, and load force $F = 100$ kN. Therefore, values of the parameters determining the cross section proportions are constant. i.e. $x_1 = 0.0882$ and $x_2 = 0.045$, while the relative length λ varies in the range ($10 \leq \lambda \leq 40$).

The results of the calculation are presented in the Table 1.

Table 1. The values of deflection and stresses for the I-beam – the analytical – sandwich theory.

λ	10	15	20	25	30	40
$w_{\max}^{(A-S)}$ [mm]	1.23	3.59	8.04	15.27	25.98	60.62
$\sigma_{\max}^{(A-S)}$ [MPa]	118.0	156.5	195.0	233.5	271.9	348.9
$\tau_{\max}^{(A-S)}$ [MPa]	31.5	31.5	31.5	31.5	31.6	31.6
$\tau_{\min}^{(A-S)}$ [MPa]	28.8	28.8	28.9	28.9	28.9	29.0

Table 2. The values of deflection and stresses for the I-beam – the classical beam theory.

λ	10	15	20	25	30	40
$w_{\max}^{(E-B)}$ [mm]	0.928	3.133	7.426	14.503	25.061	59.406
$\sigma_{\max}^{(E-B)}$ [MPa]	77.1	115.6	154.2	192.7	231.3	308.3
$\tau_{\max}^{(G-T)}$ [MPa]	31.2	31.2	31.2	31.2	31.2	31.2
$\tau_{\min}^{(G-T)}$ [MPa]	28.0	28.0	28.0	28.0	28.0	28.0

The ratio of the deflection calculated in accordance with the analytical – sandwich theory to the one obtained with the classical beam theory is equal to

$$(3.16) \qquad \frac{w_{\max}^{(A-S)}}{w_{\max}^{(E-B)}} = 48C_{ww} \sum_k \widetilde{w}_k \sin^2\left(\frac{\pi}{2}k\right).$$

In case of shorter beams, i.e. for small λ values, the ratio exceeds unity. It means that the deflection of a short beam is higher as compared to the value provided by the classical theory. The difference between the deflection values calculated according to both these theories drops with growing λ value. The effect is shown in Fig. 3.
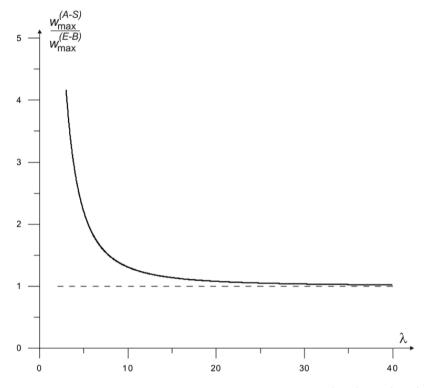

FIG. 3. Comparison of the deflections calculated in accordance with (A-S) and (E-B) theories *versus* λ.

Similar ratio of the normal stresses calculated with the use of both above mentioned theories is equal to

$$(3.17) \qquad \frac{\sigma_{\max}^{(\text{Sandwich})}}{\sigma_{\max}^{(E-B)}} = \frac{8C_{ww}}{1 + 2x_1} \sum_k \widetilde{\sigma}_k \sin^2\left(\frac{\pi}{2}k\right).$$

The deviation between the normal stress values so obtained is still higher than for the deflections, however, it also drops with growing λ. It is depicted in Fig. 4.
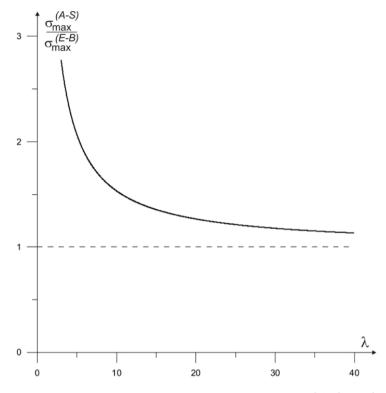
Fig. 4. Comparison of normal stresses calculated in accordance with (A-S) and (E-B) theories *versus* λ.

4. FEM model and numerical calculations

In order to confirm the theoretical results the beams have been modeled with a view to calculate the deflections and stresses with the FEM method, using the SolidWorks software. Because of symmetry of the problem only a half of the beam has been considered with proper boundary conditions imposed on the symmetry planes.

5. SolidWorks analysis

The analysis was carried out with the use of the SolidWorks software. The meshes have been built of solid tetrahedral elements (with four Jacobian points). Basic dimensions and parameters of the beam are identical to those of Table 3, except that the values of the beam length varied according to the ones specified in Tables 1 and 2, for $\lambda = 10, 15, 20, 25, 30, 40$, with a view to provide more comprehensive comparison of the results.

Table 3. Dimensions of the beam for $\lambda = 10$.

Dimension	Value
Length L ($\lambda = 10$)	1700
Depth H [mm]	200
Depth of the web a [mm]	170
Width of the web b [mm]	200
Thickness of the web t_w [mm]	9
Thickness of the flanges t_f [mm]	15
Young's modulus of the core E [MPa]	200
Poisson ratio of the core υ	0.3

The pattern of normal stress occurring in the middle cross-section of the I-beam for $\lambda = 10$ is shown in Fig. 5. Maximum stress value amounts to 118.4 MPa.
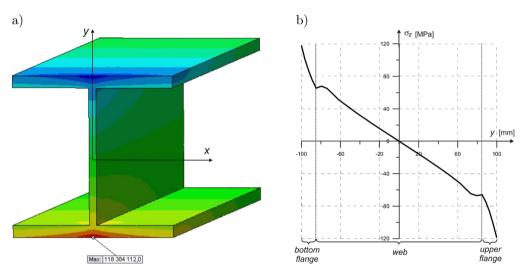

FIG. 5. Illustration of normal stress σ_z arising in the middle cross-section of the I-beam for $\lambda = 10$: a) only a half of the beam is shown, with its middle cross-section in the front part of the picture, b) the plot of the σ_z stress along the y-axis.

The plot of the σ_z stress arising along the web middle line, i.e. the y-axis (Fig. 5b), shows a disturbance of the stress at the boundary between the flanges and the web.

On the other hand, the pattern of shear stress acting in the web cross-section located at certain distance from the middle of the I-beam for $\lambda = 10$ is shown in Fig. 6. Maximum stress value amounts to 31.22 MPa.

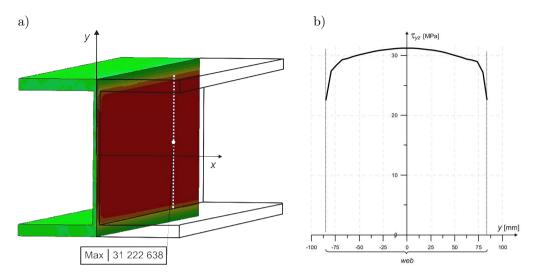Deflection of the I-beam for $\lambda = 10$ is depicted in Fig. 7.

a)

Max | 31 222 638

b)

FIG. 6. Illustration of shear stress τ_{yz} arising in the web cross-section of the I-beam located beyond its middle for $\lambda = 10$: a) only a half of the beam, partially transparent, is shown, with its middle cross-section in the front part of the picture, b) the plot of the τ_{yz} stress along the line parallel to y-axis and located at the longitudinal plane of beam symmetry.
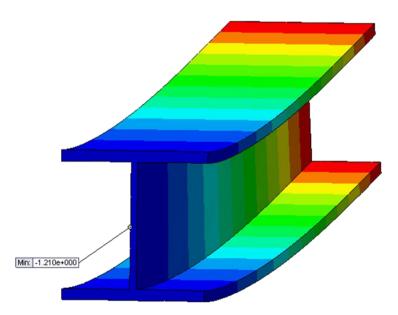

Min: | -1.210e+000

FIG. 7. Illustration of the I-beam deflection for $\lambda = 10$.

The values of stresses and deflections obtained with the help of SolidWorks for higher for $\lambda =$ values are not shown in figures, nevertheless, all the results for all the considered variants are presented in Table 4.

Table 4. The values of deflection and stresses for the I-beam – the SolidWorks FEM solutions.

λ	10	15	20	25	30	40
$w_{\max}^{(SW)}$ [mm]	1.21	3.47	7.73	14.63	24.85	57.88
$\sigma_{\max}^{(SW)}$ [MPa]	118.4	157.4	195.1	233.7	272.7	348.4
$\tau_{\max}^{(SW)}$ [MPa]	31.22	31.23	31.22	31.26	31.23	31.25
$\tau_{\min}^{(SW)}$ [MPa]	22.5	21.3	21.2	20.6	21.86	22.1

6. Comparison of the analytical and FEM-numerical results

The analytical and FEM-numerical results may be compared based on the Tables 1 and 4. The FEM analysis satisfactorily confirms the analytical results, giving evidence that in case of shorter beams the values of deflection and stresses clearly deviate from the ones provided by the classical beam theory.

The calculation carried out with the help of SolidWorks shows that the per cent deviation between the deflection values varies from 1.6 for $\lambda = 10$ to 4.5 for $\lambda = 40$. On the other hand, compliance between maximum normal stress is much better, as it varies from 0.34 per cent for $\lambda = 10$ to 0.15 per cent for $\lambda = 40$. Maximum shear stresses also very well comply in all the variants. This is not the case for the minimum shear stress, but it should be noticed that it is only a local effect. The minimum stresses specified in Table 5 are calculated in the web points adjacent to the flange. In very small distance from the flange the stress grows to the value approximating its analytical estimation.

7. Conclusions

The hypothesis that initially plane cross-section of a beam remains plane after bending leads to omission of the shear effect. In case of long beams (i.e. for higher λ values) the shear effect becomes small and may be omitted. Otherwise, in order to calculate properly the deflection and stresses in a bent beam this hypothesis must be revised. The assumption of the analytical – sandwich theory, in which the cross section deforms as is presented in Fig. 2b and according to subsequent formulae, enables to formulate a new approach to the problem that is much more effective in case of shorter beams.

It should be noticed that real beams used in most of mechanical structures should be rather considered as short ones, with the λ values usually below 20.

Figures 3 and 4 illustrate the difference between these two approaches, which is additionally confirmed by the FEM computation carried out with the Solid-Works software. It was found that the difference between analytical and numeri-

cal FEM results is below 4.5 percent in case of deflections and below 0.34 percent for the stresses.

The proposed sandwich model of the I-beam accurately describes the shear effect arising in the beam. This effect has been displayed based on the Timoshenko beam theory (HUTCHINSON [3] and BECK and SILVA Jr. [11]).

REFERENCES

1. GERE J.M., TIMOSHENKO S.P., *Mechanics of materials*, PWS-KENT Pub. Comp., Boston 1984.

2. WANG C.M., REDDY J.N., LEE K.H., *Shear deformable beams and plates*, Elsevier, Amsterdam, Lausanne, New York, Oxford, Tokyo 2000.

3. HUTCHINSON J.R., *Shear coefficients for Timoshenko beam theory*, ASME Journal of Applied Mechanics, **68**(1): 87–92, 2001.

4. SONG O., LIBRESCU L., JEONG N-H., *Static response of thin-walled composite I-beams loaded at their free-end cross-section: Analytical Solution*, Composite Structures, **52**(1): 55–65, 2001.

5. JUNG S.N., LEE J-Y., *Closed form analysis of thin-walled composite I-Beams considering non-classical effect*, Composite Structures, **60**(1): 9–17, 2003.

6. EL FATMI R., *Non-uniform warping including the effects of torsion and shear forces, Part I: A general beam theory*, International Journal of Solids and Structures, **44**(18–19): 5912–5929, 2007.

7. ROMANOFF J., VARSTA P., *Bending response of web-core sandwich plates*, Composite Structures, **81**(2): 292–302, 2007.

8. BLAAUWENDRAAD J., *Shear in structural stability: On the Engesser-Haringx discord*, ASME Journal of Applied Mechanics, **77**(3): 031005, 2010.

9. DONG S.B., ALPDOGAN C., TACIROGLU E., *Much ado about shear correction factors in Timoshenko beam theory*, International Journal of Solids and Structures, **47**(13): 1651–1665, 2010.

10. SHI G., VOYIADJIS G.Z., *A sixth-order theory of shear deformable beams with variational consistent boundary conditions*, ASME Journal of Applied Mechanics, **78**(2): 021019, 2010.

11. BECK A.T., DA SILVA JR C.R.A., *Timoshenko Versus Euler Beam Theory: Pitfalls of a deterministic approach*, Structural Safety, **33**(1): 19–25, 2011.

12. KIM N-I., *Shear deformable doubly- and mono-symmetric composite I-beams*, International Journal of Mechanical Sciences, **53**(1): 31–41, 2011.

13. MAGNUCKA-BLANDZI E., *Dynamic stability and static stress state of a sandwich beam with metal foam core using three modified Timoshenko hypothesis*, Mechanics of Advanced Materials and Structures, **18**(2): 147–158, 2011.

14. MAGNUCKA-BLANDZI E., *Mathematical modelling of a rectangular sandwich plate with a metal foam core*, Journal of Theoretical and Applied Mechanics, **49**(2): 439–455, 2011.

15. SHI G., WANG X., *A constraint on the consistence of transverse shear strain energy in the higher-order shear deformation theories of elastic plates*, ASME Journal of Applied Mechanics, **80**(4): 044501, 2013.

16. Li S., Wan Z., Wang X., *Homogenized and classical expressions for static bending solutions for functionally graded material Levinson beams*, Applied Mathematics and Mechanics – Engl. Ed., **36**(7): 895–910, 2015.

17. Magnucka-Blandzi E., Magnucki K., Wittenbeck L., *Mathematical modeling of shearing effect for sandwich beams with sinusoidal corrugated cores*, Applied Mathematical Modelling, **39**(9): 2796–2808, 2015.

18. Urbański A., *Analysis of a beam cross-section under coupled actions including transversal shear*, International Journal of Solids and Structures, **71**: 291–307, 2015.

19. Magnucki K., Malinowski M., Magnucka-Blandzi E., Lewinski J., *Three-point bending of a short beam with symmetrically varying mechanical properties*, Composite Structures, **179**: 552–557, 2017.

20. Schulz M., *Beam element with a 3D response for shear effects*, Journal of Engineering Mechanics, **144**(1): 04017149, 2017.